



1 The impact of RCM formulation and resolution on
2 simulated precipitation in Africa

3
4 Minchao Wu¹, Grigory Nikulin¹, Erik Kjellström¹, Danijel Belušić¹, Colin Jones² and David
5 Lindstedt¹

6 Correspondence to: Minchao Wu (minchaowu.acd@gmail.com)

7

8 ¹Swedish Meteorological and Hydrological Institute, Folkborgsvägen 17, 60176 Norrköping,
9 Sweden

10 ²National Centre for Atmospheric Science (NCAS), University of Leeds, Leeds, UK

11

12

13

14

15

16

17

18

19

20

21



22

Abstract

23 We investigate the impact of model formulation and horizontal resolution on the ability of
24 Regional Climate Models (RCMs) to simulate precipitation in Africa. Two RCMs - SMHI-RCA4
25 and HCLIM38-ALADIN are utilized for downscaling the ERA-Interim reanalysis over Africa at
26 four different resolutions: 25, 50, 100 and 200 km. Additionally to the two RCMs, two different
27 configurations of the same RCA4 are used. Contrasting different RCMs, configurations and
28 resolutions it is found that model formulation has the primary control over many aspects of the
29 precipitation climatology in Africa. Patterns of spatial biases in seasonal mean precipitation are
30 mostly defined by model formulation while the magnitude of the biases is controlled by
31 resolution. In a similar way, the phase of the diurnal cycle is completely controlled by model
32 formulation (convection scheme) while its amplitude is a function of resolution. Although higher
33 resolution in many cases leads to smaller biases in the time mean climate, the impact of higher
34 resolution is mixed. An improvement in one region/season (e.g. reduction of dry biases) often
35 corresponds to a deterioration in another region/season (e.g. amplification of wet biases). The
36 experiments confirm a pronounced and well known impact of higher resolution - a more realistic
37 distribution of daily precipitation. Even if the time-mean climate is not always greatly sensitive
38 to resolution, what the time-mean climate is made up of, higher order statistics, is sensitive.
39 Therefore, the realism of the simulated precipitation increases as resolution increases.
40 Our results show that improvements in the ability of RCMs to simulate precipitation in Africa
41 compared to their driving reanalysis in many cases are simply related to model formulation and



42 not necessarily to higher resolution. Such model formulation related improvements are strongly
43 model dependent and in general cannot be considered as an added value of downscaling.

44

45 Keywords: RCA4, HCLIM, Resolution dependency, Added value, CORDEX-Africa

46

47

48

49

50

51

52

53

54

55

56

57

58

59

60

61



62

1 Introduction

63 Regional climate modeling is a dynamical downscaling method widely used for downscaling
64 coarse-scale global climate models (GCMs) to provide richer regional spatial information for
65 climate assessments and for impact and adaptation studies (Giorgi and Gao, 2018; Giorgi and
66 Mearns, 1991; Laprise, 2008; Rummukainen, 2010). It is well-established that regional climate
67 models (RCMs) are able to provide added value (understood as improved results) compared to
68 their driving GCMs. This includes better representation of regional and local weather and climate
69 features as a result of better capturing small-scale processes, including those influenced by
70 topography, coast lines and meso-scale atmospheric phenomena (Flato et al., 2013; Prein et al.,
71 2016). However, added value from RCMs may have different causes and it may not always be
72 for the right reason where “right reason” would result from an improved representation of
73 regional process at smaller scales. Such improvement leads to more accurate results on local
74 scales, and can, to some extent, also reduce large-scale GCM biases (Caron et al., 2011;
75 Diaconescu and Laprise, 2013; Sørland et al., 2018). Contrastingly, added value may be
76 attributed to the “wrong reason”, not directly related to higher resolution in RCMs but to
77 different model formulation in the RCMs and their driving GCMs. It is possible that the physics
78 of a RCM has been targeted for processes specific to the region it is being run for, giving it a
79 local advantage over GCMs that may have had their physics developed for global application.
80 However, it is questionable if improvements of such “downscaling” via physics can be
81 considered as an added value. In general, RCMs can either reduce or amplify GCM biases
82 sometimes even changing their signs (Chan et al., 2013).



83 Issues as those mentioned above, have raised substantial concerns among regional climate
84 modelers (e.g., Castro, 2005; Xue et al., 2014). It has been pointed out that understanding of the
85 added value remains challenging. It would become even more complicated taking into account
86 the effects of different realizations, such as the size of domain, lateral boundary conditions,
87 geographical location, model resolution and its internal variability (Di Luca et al., 2015; Hong
88 and Kanamitsu, 2014; Rummukainen, 2016). All the above factors potentially influence
89 downscaled results leading to different interpretation of the downscaling effects, thus the
90 robustness of added value. For example, it was shown that over the Alps, downscaling with
91 multiple RCMs at increasing resolutions in general is able to provide a more realistic
92 precipitation pattern than the forcing GCMs, and it is regarded as added values from RCMs
93 (Torma et al., 2015b). Similarly, Lucas-Picher et al (2017) found added value over the Rocky
94 Mountains, another region with strong topographic influence on hydrological processes.
95 However, the results are not unambiguous and sometimes limited added value is found when
96 comparing to the forcing data, (e.g. Wang and Kotamarthi, 2014) over North America. This
97 implies that the understanding of downscaling effects is context-dependent and one should
98 carefully interpret the downscaled results in order to detect robust added value.

99 Africa is foreseen to be vulnerable to future climate change, which early on inspired efforts to
100 employ RCMs for impact and adaptation studies (e.g. Challinor et al., 2007). Further to previous
101 coordinated downscaling activities over Africa as for example the African Monsoon
102 Multidisciplinary Analyses (AMMA) (Van der Linden and Mitchell, 2009), the Coordinated
103 Regional climate Downscaling Experiment (CORDEX) provides a large ensemble of RCM
104 projections for Africa (Giorgi et al., 2009; Jones et al., 2011). All CORDEX RCMs follow a



105 common experiment protocol including a predefined domain at 50km resolution and common
106 output variables and format that facilitates assessment of projected climate changes in Africa.
107 Under this framework, RCMs at 50-km horizontal resolution are found to have the capability of
108 providing added value in representing African climatological features compared to their forcing
109 GCMs, which generally have the resolution coarser than 100 km (Dosio et al., 2015;
110 Moufouma-Okia and Jones, 2015; Nikulin et al., 2012). However, a number of common
111 problems with the RCMs are identified, which include, for example, dry biases over
112 convection-dominated regions like the Congo basin, too early onset of the rainy season for the
113 West African Monsoon region and biases in representing the diurnal cycle of precipitation (Kim
114 et al., 2014; Laprise et al., 2013; e.g. Nikulin et al., 2012). So far, it is still not clear if differences
115 between the CORDEX Africa RCMs and their driving GCMs are related to higher RCM
116 resolution or to RCM internal formulation, or to the combination of both. A thorough
117 understanding of such differences and of added value of the CORDEX-Africa RCMs is
118 necessary for robust regional assessments of future climate change and its impacts in Africa.

119 In this study, we aim to separate the impact of model formulation and resolution on the ability of
120 RCMs to simulate precipitation in Africa. We conduct a series of sensitivity, reanalysis-driven
121 experiments by applying two different RCMs, one of them in two different configurations, at
122 four horizontal resolutions. Contrasting the different experiments allow us to separate the impact
123 of model formulation and resolution. We present an overview and the first results of the
124 experiments conducted and leave in-depth detailed process studies for different regions to
125 forthcoming papers.



126

2 Methods and Data

127

2.1 The Regional Climate Models

128

2.1.1 RCA4

129

The Rossby Centre Atmosphere regional climate model - RCA (Jones et al., 2004; Kjellström et

130

al., 2005; Räisänen et al., 2004; Rummukainen et al., 2001; Samuelsson et al., 2011) is based on

131

the numerical weather prediction model HIRLAM (Undén et al. 2002). To improve model

132

transferability, the latest fourth generation of RCA, RCA4, has a number of modifications for

133

specific physical parameterizations. This includes the modification of convective scheme based

134

on Bechtold-Kain-Fritsch scheme (Bechtold et al., 2001) with revised calculation of convective

135

available potential energy (CAPE) profile according to Jiao and Jones (2008), and the

136

introduction of turbulent kinetic energy (TKE) scheme (Lenderink and Holtslag, 2004). The

137

RCA4 model has been applied in many regions worldwide, among them Europe (Kjellström et

138

al., 2016, 2018; Kotlarski et al., 2015), the Arctic (Berg et al., 2013; Koenigk et al., 2015; Zhang

139

et al., 2014), Africa (Nikulin et al., 2018; Wu et al., 2016), South America (Collazo et al., 2018;

140

Wu et al., 2017), South-East (Tangang et al., 2018) and South Asia (Iqbal et al., 2017).

141

In addition to the standard RCA4 configuration, used in CORDEX, in this study we also include

142

a RCA configuration with reduced turbulent mixing in stable situations (especially momentum

143

mixing). Such change in model formulation was applied to reduce a prominent dry bias found in

144

RCA4 CORDEX Africa simulations over Central Africa (Tamoffo et al., 2019; e.g. Wu et al.,

145

2016). Using two configurations of RCA4 allows us to examine how sensitive our results are to



146 different formulations of the same model. We hereafter denote the original RCA4 configuration
147 as RCA4-v1 and the new one as RCA4-v4.

148 2.1.2 HCLIM

149 HARMONIE-Climate (HCLIM) is a regional climate modelling system designed for a range of
150 horizontal resolutions from tens of kilometers to convection permitting scales of 1-3km
151 (Belušić et al., 2019; Lindstedt et al., 2015). It is based on the ALADIN-HIRLAM numerical
152 weather prediction system (Belušić et al., 2019; Bengtsson et al., 2017; Termonia et al., 2018).
153 The HCLIM system includes three atmospheric physics packages AROME, ALARO and
154 ALADIN, which are designed for different horizontal resolutions. The ALADIN model
155 configuration used in this study employs the hydrostatic ARPEGE-ALADIN dynamical core
156 (Temperton et al., 2001), a mass-flux scheme based on moisture convergence closure for
157 parameterizing deep convection (Bougeault, 1985) and SURFEX as the surface scheme (Masson
158 et al., 2013). All details about the version of HCLIM used in this study (HCLIM38), and its
159 applications over different regions can be found in (Belušić et al., 2019). We need to note that
160 HCLIM38-ALADIN used in the study is not the same model as ALADIN-Climate used in
161 CORDEX (Daniel et al., 2019). We refer to HCLIM38-ALADIN as HCLIM-ALADIN hereafter.

162

2.2 Experimental design

163 To investigate the response of both RCA4 and HCLIM-ALADIN to horizontal resolution, we
164 conduct a set of sensitivity experiments driven by the ERA-Interim reanalysis (denoted as
165 ERAINT hereafter; Dee et al., 2011) at four different resolutions. These resolutions are 1.76,
166 0.88, 0.44 and 0.22° for RCA4 with the rotated coordinate system and 200, 100, 50 and 25km for



167 HCLIM-ALADIN with the Lambert Conformal projection. The 0.44° or 50km resolution is
168 recommended by the CORDEX experiment design and used in the CORDEX-Africa ensemble.
169 Hereafter, the resolution in kilometers is used unless otherwise specified. The setup of the
170 simulations at the four resolutions is identical apart from the timestep that is adjusted to ensure
171 numerical simulation stability and the size of the full computational domain with the relaxation
172 zone (see Table 1). The relaxation zone has 8 grid-points in all directions and increases (in km) at
173 coarser resolution while the interior CORDEX-Africa domain is the same. Larger size of the
174 computational domain at coarser resolution may have a potential impact on the results leading to
175 larger internal variability developed by the RCMs and weaker constraints on the ERAINT
176 forcing. We perform an additional experiment with RCA4 at 0.88° resolution taking the full
177 computational domain from the 1.76° RCA simulation. For precipitation differences between the
178 two experiments are at the noise level while for seasonal mean temperature it can be up to 1°C.
179 The RCA4 0.88° simulations and the HCLIM-ALADIN 100km one represent a slight upscaling
180 of ERAINT (about 0.7° or about 77km at the Equator) and we refer to them as “no added value
181 experiment”. No resolution-dependent added value of the RCMs is expected for these
182 simulations and all differences between the RCMs and their driving ERAINT are attributed to
183 different model formulations. We note that in general, both regional models - RCA and
184 HCLIM-ALADIN were developed to operate at a range of 10-50km resolution and their
185 performance at 100 and 200km may not be optimal. All simulations are conducted without
186 spectral nudging and analysis is done for the CORDEX-Africa domain shown in Fig. 1.

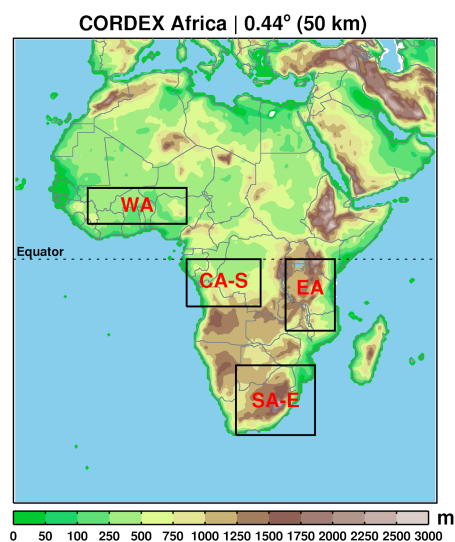
187

188 Table 1. Details of the RCA4 and HCLIM ALADIN experiments



Experiment name	Horizontal resolution (deg. / km)	Domain size (lon × lat)	Geographical area (deg.)		Time step (sec)
			South, North	West, East	
RCA4-v* 1.76°	1.76°	66 × 67	-60.5, 55.66	-38.06, 76.34	1200
RCA4-v* 0.88°	0.88°	126 × 121	-54.78, 50.82	-33.22, 76.78	1200
RCA4-v* 0.44°	0.44°	222 × 222 ^a	-50.16, 47.08	-29.04, 68.20	1200
RCA4-v* 0.22°	0.22°	406 × 422	-48.07, 44.55	-26.95, 62.15	600
HCLIM-ALADIN 200km	200 km	80 × 90	-58.34, 56.71	-46.98, 82.98	1800
HCLIM-ALADIN 100km	100 km	128 × 150	-53.89, 51.70	-37.01, 73.01	1800
HCLIM-ALADIN 50km	50 km	240 × 270	-51.56, 48.98	-35.85, 71.85	1200
HCLIM-ALADIN 25km	25 km	450 × 512	-50.43, 47.73	-33.64, 69.64	600

189
 190



191 **Figure 1** Topography (m) for the the CORDEX-Africa domain in RCA4 at 50km resolution. Boxes
 192 indicate the four subregions used for spatially averaged analysis: West Africa (WA), East Africa (EA), the
 193 southern Central Africa (CA-S), and eastern southern Africa (SA-E).



194

2.3 Observations and reanalysis

195 Observational datasets in Africa, in general, agree well for large-scale climate features but can
196 deviate substantially at regional and local scales (Fekete et al., 2004; Gruber et al., 2000; Nikulin
197 et al., 2012). To take into account the observational uncertainties, we utilize a number of gridded
198 precipitation datasets. They include three gauged-based datasets: the Global Precipitation
199 Climatology Centre, GPCC, version 7 (Schneider et al., 2014), the Climate Research Unit
200 Time-Series, CRU TS, version 3.23 (Harris et al., 2014), and University of Delaware, UDEL,
201 version 4.01 (Legates and Willmott, 1990). All these three datasets are at 0.5° horizontal
202 resolution. For the evaluation of precipitation extremes and diurnal cycle simulated by RCMs,
203 we utilize a satellite-based precipitation dataset from the Tropical Rainfall Measuring Mission,
204 TRMM 3B42 version 7 (Huffman et al., 2007), which is at 0.25° horizontal resolution and
205 3-hourly temporal resolution. ERAINT as the driving reanalysis is also used for analysis. In
206 contrast to climate models, ERAINT precipitation is a short term forecast product and there are
207 several ways to derive ERAINT precipitation (e.g. different spin-up, base time and forecast
208 steps) that can lead to different precipitation estimates (Dee et al. 2011). ERAINT precipitation is
209 derived by the simplest method, without spinup as in some of the previous studies (Dosio et al.,
210 2015; Moufouma-Okia and Jones, 2015; Nikulin et al., 2012): 3-hourly precipitation uses the
211 base times 00/12 and forecast steps 3/6/9/12 hours, while daily precipitation uses base times
212 00/12 and forecast steps of 12 hours. The RCMs and ERAINT represent 3-hourly mean
213 precipitation for the 00:00-03:00, 03:00-06:00, ... 21:00-00:00 intervals while TRMM
214 precipitation averages represent approximately the 22:30-01:30, 01:30-04:30, ... 19:30-22:30
215 UTC intervals.



216

2.4 Methods

217 The coarsest resolution 200 km is used as a reference resolution for spatial maps. The
218 higher-resolution simulations are aggregated to the 200 km grid by the first-order conservative
219 remapping method (Jones, 1999). In this way we expect that the difference among the aggregated
220 results at common resolution should mainly be caused by the different treatment for fine-scale
221 processes (Di Luca et al., 2012). For the regional analysis, such as the analysis of annual cycle,
222 diurnal cycle and daily precipitation intensity, we focus on four subregions, presenting different
223 climate zones in Africa: West Africa (10°W~10°E, 7.5°N~15°N), East Africa (30°E~40°E,
224 15°S~0°S), the southern Central Africa (10°E~25°E, 10°S~0°S), and the eastern South Africa
225 (20°E~36°E, 35°S~22°S) as defined in Fig. 1. The period 1981-2010 is used for the analysis in
226 this study, unless otherwise specified.

227

3 Results and Discussion

228

3.1 Seasonal mean

229 In the boreal summer defined here as July-September (JAS), the tropical rain belt (TRB)
230 associated with the intertropical convergence zone (ITCZ) is positioned to its most northern
231 location with the maximum precipitation north of the Equator (Fig. 2a). CRU, UDEL and GPCC
232 aggregated to the 200km resolution, generally agree well with each other, with only slight local
233 differences (Fig. 2a-c). ERAINT overestimates precipitation over Central Africa and along the
234 Guinea Coast while underestimates it over West Africa, north of the Guinea Coast (Fig. 2d). All
235 RCA4-v1 simulations have a pronounced dry bias (Fig. 2e-h) that spatially almost coincides with

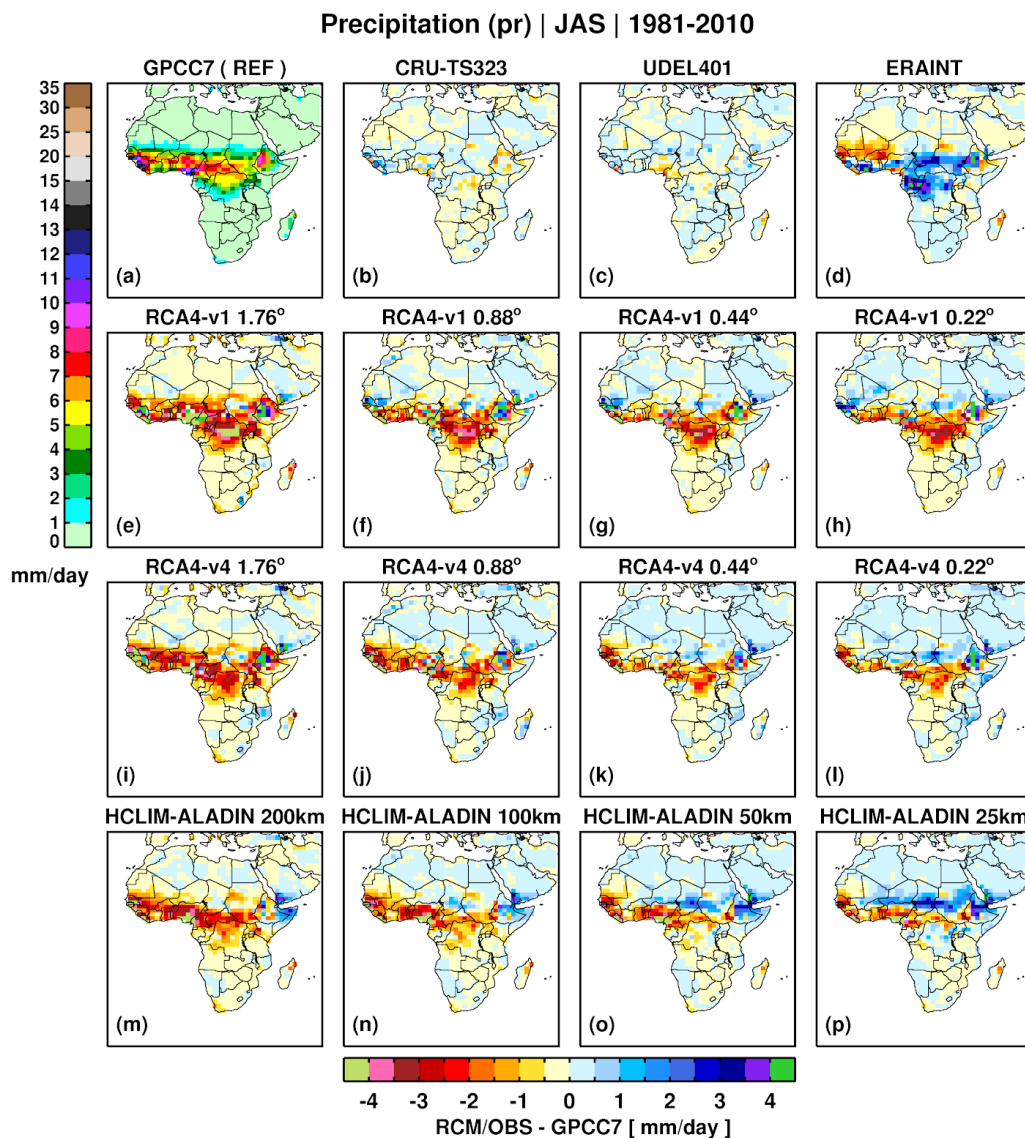


236 the wet bias in ERAINT and increases at coarser resolution (Fig1e-f). RCA4-v4 shows a similar
237 bias pattern compared to RCA4-v1 but substantially reduces the dry bias over Central Africa at
238 all four resolutions (Fig. 2i-l). For both configurations of RCA4, the smallest dry bias is found at
239 the highest 25km resolution, although an overestimation of precipitation north of the dry bias
240 becomes more pronounced, especially for RCA4-v4. HCLIM-ALADIN, in general, shows some
241 similarities to RCA4 with a pronounced dry bias in West and Central Africa at 200km that is
242 strongly reduced with increasing resolution. However, a wet bias emerges on the northern flank
243 of the rain belt at 50 and 25km. For JAS there is a common tendency for both RCMs to generate
244 more precipitation at higher resolution leading to a reduction of the dry biases over Central
245 Africa. Such bias reduction may be considered as an resolution-related improvement. However,
246 the RCM simulations clearly show that the added value of higher resolution can be region
247 dependent. An improvement of the simulated precipitation climatology over one region
248 corresponds to deterioration of the climatology over another region. Moufouma-Okia and Jones
249 (2015) found a mixed response to resolution in simulated seasonal mean precipitation over West
250 Africa. Their RCM simulations at 50 and 12km bear a great deal of similarity with each other
251 while a simulation at 25km shows wetter conditions in the Sahel and drier ones near the coastal
252 area in the south (see their Fig. 8). In contrast, Panitz et al. (2014) found almost no difference in
253 seasonal rainfall over West Africa between two RCM simulations at 50 and 25km. We conclude
254 that for both RCA4 and HCLIM-ALADIN, spatial bias patterns are similar and more related to
255 model formulation while magnitude of biases are more sensitive to resolution. For example, the
256 sign of the bias pattern in our no added value RCM simulations at 100km in JAS (Fig. 2f, j, n) is
257 almost opposite to the sign of the bias pattern in the driving ERAINT (Fig. 2d).



258

259



260 **Figure 2.** GPCC7 mean JAS precipitation for 1981–2010 and differences compared to GPCC7 in (b-d) the
 261 other gridded observations, (e-h) the RCA4-v1, (i-l) RCA4-v4 and (m-p) HCLIM-ALADIN simulations.
 262



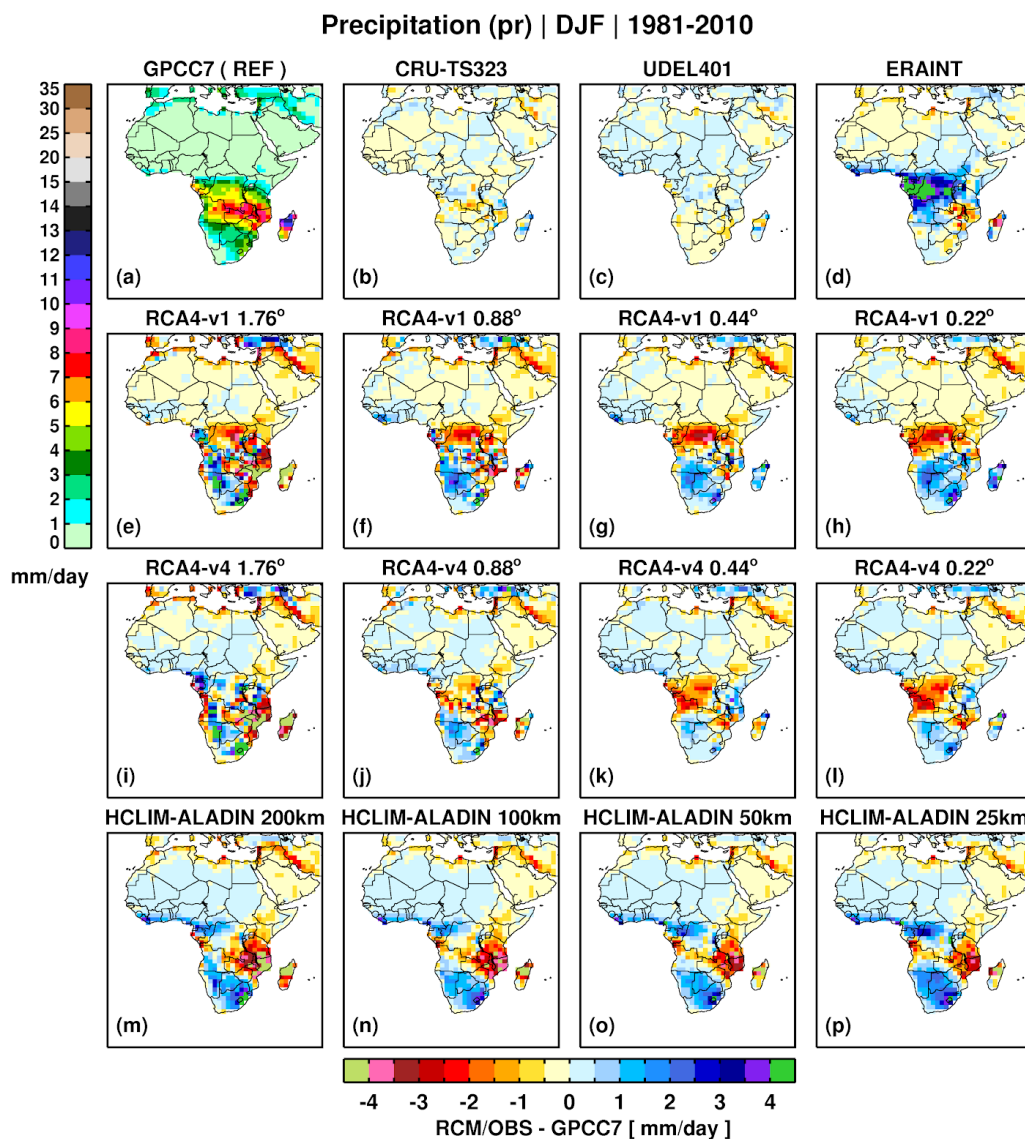
263 In boreal winter (December-February, DJF), the TRB migrates to its most southerly position
264 covering the latitudes from southern to Central Africa, with the maximum over southern tropical
265 Africa and Madagascar (Fig. 3a). Similar to JAS, observational uncertainties are generally small
266 in DJF and there is a pronounced wet bias in ERAINT over Central Africa (Fig. 3d). At 25 and
267 50km RCA4-v1 has a dipole bias pattern with an underestimation of rainfall over Central Africa
268 and an overestimation over southern Africa. At 200km there is a pronounced deterioration in the
269 simulated rainfall: a strong dry bias appears along the eastern coast and Madagascar while the
270 wet bias is amplified over large parts of southwestern Africa. At 25 and 50km RCA4-v4 shows a
271 large-scale dipole bias pattern similar in some degree to RCA4-v1. The RCA4-v4 biases are
272 smaller than the RCA4-v1 ones showing an impact of the re-tuning (reducing mixing in the
273 boundary layer). The behaviour of RCA4-v4 at coarser resolution is also similar to RCA4-v1. A
274 similar strong dry bias is emerging along the eastern coast at 200km. However, in contrast to
275 RCA4-v1, the dry bias over the Democratic Republic of Congo almost completely disappears at
276 both 100 and 200km. HCLIM-ALADIN simulates almost the same bias pattern at all resolutions,
277 strongly underestimating rainfall over southeastern Africa and overestimating it over the Guinea
278 Coast, parts of central Africa and southern Africa. There is a tendency to an increase in
279 precipitation with higher resolution in HCLIM-ALADIN: the wet biases are amplified and the
280 dry biases are reduced. Both RCA4 and HCLIM-ALADIN show a common feature -
281 intensification of the dry bias along the eastern coast of Africa at 200km. Even, if both RCMs
282 have this dry bias in common, there are also differences showing the importance of model
283 formulation. HCLIM-ALADIN has about the same bias pattern at all four resolutions while the
284 RCA4 bias pattern substantially changes across the resolutions. Such resolution dependency in



285 RCA4 may be related to the fact that RCA4 is based on a limited area model and not developed
286 to operate at 100-200km resolution. Contrastingly, HCLIM-ALADIN that is based on a global
287 model shows more consistent results even at 100-200km resolution. Although, we also note that
288 the resolution dependency of the RCA4 bias pattern over southern Africa is similar to that found
289 for the CMIP5 GCMs (Munday and Washington, 2018). They show that the GCMs with the
290 coarsest resolution and respectively the lowest topography have the wettest bias over the
291 Kalahari basin and the driest bias over the southeast Africa coast, the Mozambique Channel and
292 Madagascar. Such a bias pattern is related to a smoother barrier to northeasterly moisture
293 transport from the Indian Ocean that penetrates across the high topography of Tanzania and
294 Malawi into subtropical southern Africa. However, in our analysis, HCLIM-ALADIN does not
295 show such resolution-related dependency. In general, similar to JAS, the added value of higher
296 resolution in DJF is region dependent: with higher resolution biases are reduced over one region
297 but amplified over another.



298



299 **Figure 3.** As Fig. 2, but for DJF.

300

3.2 Annual cycle

301 The annual cycle of precipitation over the four subregions is shown in Fig. 4. The observed

302 annual cycle of precipitation over West Africa depicts the West African Monsoon (WAM)



303 rainfall, with maximum precipitation in August (Fig. 4a). All observational datasets and
304 ERAINT agree well with each other with only a small underestimation of rainfall by ERAINT in
305 June-August. In contrast to the observations, RCA4-v1 has a bimodal annual cycle with a too
306 early onset of the rainy season (Fig. 4b). The simulated rainfall is overestimated in March-May,
307 underestimated in July-August during the active WAM period and is well in line with the
308 observations during the cessation of the WAM rainfall in September-November. RCA4-v4 shows
309 a similar behaviour but the first rainfall peak in May is reduced and the annual cycle has a more
310 unimodal shape (Fig. 4c). HCLIM-ALADIN, in general, shows similar features as both
311 configurations of RCA4, although has more similarities with RCA4-v4 (Fig. 4d). The too early
312 onset of the rainy season is a common problem for many RCMs reported by Nikulin et al.,
313 (2012). Our results show that this is not dependent on resolution but instead related to model
314 formulation. Higher resolution reduces the wet bias during the onset of the rainy season for
315 RCA-v1, has no impact for RCA-v4 and amplifies the wet bias in HCLIM-ALADIN.
316 Nevertheless, the impact of higher resolution is more consistent during the rainy season.
317 Increasing resolution tends to increase monsoon rainfall for both RCMs, resulting in smaller dry
318 biases and a pattern closer to the unimodal one in the observations. Eastern and Central Africa
319 have a bimodal annual cycle of rainfall with two peaks around November and May (Fig. 4e,i).
320 GPCC, CRU and UDEL agree well on the phase and magnitude of the annual cycle for both
321 subregions. ERAINT has a weaker bimodality overestimating precipitation in
322 December-February over Eastern Africa and all year round over Central Africa with the largest
323 wet bias during October-April. Both configurations of RCA4 fail to reproduce the bimodal
324 annual cycle in Eastern Africa at 200km underestimating precipitation all year round and

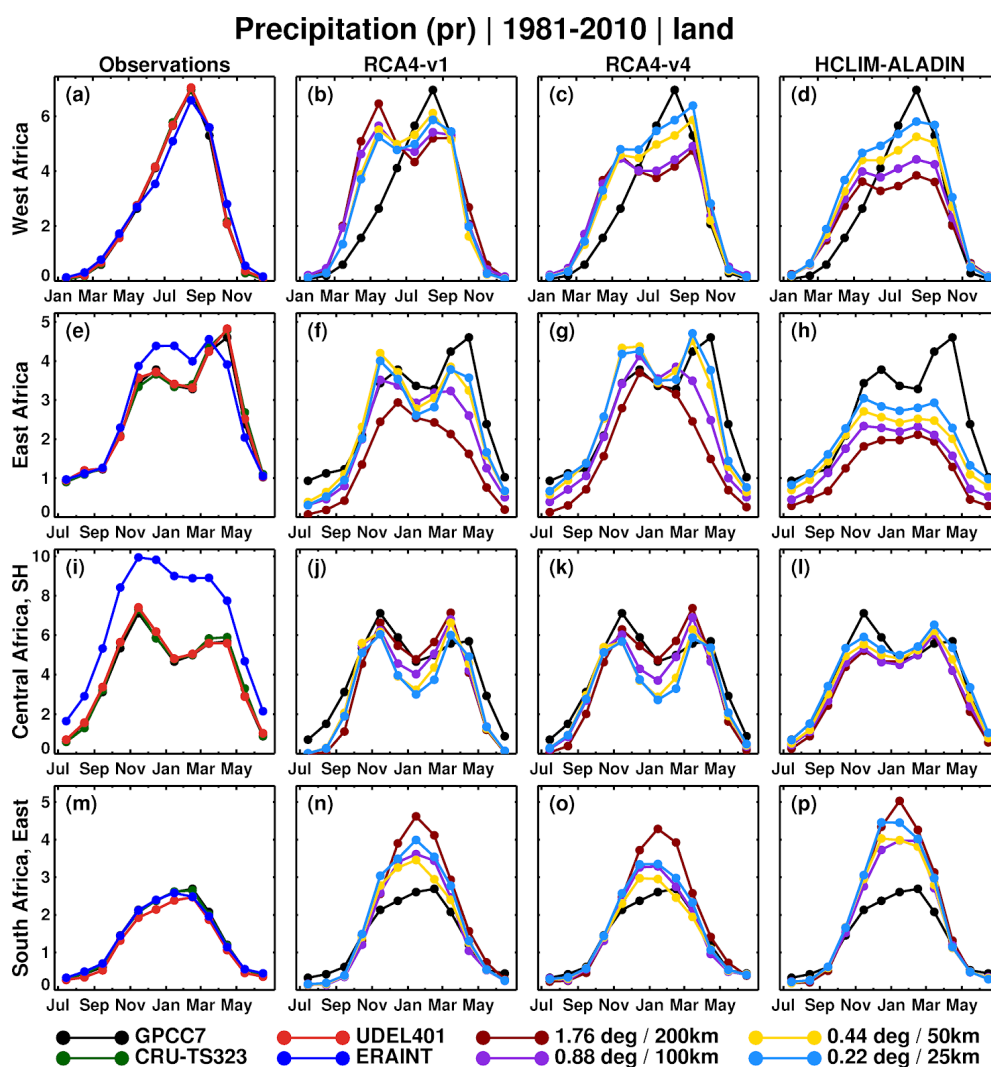


325 showing a single rainfall peak in December (Fig. 4j,k). Increasing resolution reduces the dry bias
326 and leads to an improvement in the shape of the annual cycle. The bimodal shape begins to
327 appear at 100km and becomes much closer to the observation at 50 and 25km. Despite some
328 mixed dry and wet biases in different seasons, the 25 and 50km RCA4 simulations show the best
329 agreement with the observations. In contrast to RCA4, HCLIM-ALADIN simulates the unimodal
330 annual cycle at all four resolutions and some sign of bimodality only appears at 25km (Fig. 4h).
331 Similar to RCA4, increasing resolution leads to an increase in precipitation in HCLIM-ALADIN,
332 although a dry bias is a prominent feature from November to May in all HCLIM-ALADIN
333 simulations. For Central Africa, the bimodality of the annual cycle is well reproduced by both
334 RCMs at all resolutions (Fig. 4j-l). An interesting feature is that RCA4 shows completely
335 opposite behavior in Central Africa compared to Eastern Africa. Increasing resolution leads to
336 decreasing precipitation for both configurations of RCA4 during the rainy seasons and especially
337 in January. HCLIM-ALADIN maintains similar behavior to that in Eastern Africa, although
338 difference in precipitation across the resolutions is small (Fig. 4l). Both RCMs strongly reduce
339 the ERAINT wet bias even in the no-added value experiment at 100km. Such improvement
340 indicates that model formulation plays a more important role than resolution over Central Africa.
341 For the eastern Southern Africa, the annual cycle of precipitation is unimodal with its maximum
342 in austral summer (Fig. 4m). Similar to West Africa, uncertainties between observational datasets
343 and reanalysis are small. RCA4 in general overestimates rainfall during the rainy season with the
344 largest wet bias at 200km. Surprisingly, the simulated rainfall is almost the same at 25 and
345 100km while the smallest bias is found at 50km for both RCA4 configurations.
346 HCLIM-ALADIN also overestimates precipitation during the rainy season at all four resolution



347 (Fig. 4p). However, the smallest wet bias in the HCLIM-ALADIN simulations is found at 50 and
 348 100km.

349



350 **Figure 4.** Annual cycle of precipitation over the four subregions in observations/ERAINT and as
 351 simulated by RCA4 and HCLIM-ALADIN at the four different resolutions. Only land grid boxes are used
 352 for averaging over the subregions. Units are mm/day.

353
 354
 355



356

3.3 Diurnal cycle

357 The diurnal cycle is a prominent feature of forced atmospheric variability with a strong impact
358 on regional- and local-scale thermal and hydrological regimes. The diurnal cycle of precipitation
359 in the tropics is well documented and includes a late afternoon/evening maximum over land (Dai
360 et al., 2007). However, it is still a common challenge for GCMs (Dai, 2006; e.g. Dai and
361 Trenberth, 2004; Dirmeyer et al., 2012), RCMs (e.g. Da Rocha et al., 2009; Jeong et al., 2011;
362 Nikulin et al., 2012) and reanalyses (Nikulin et al., 2012) to accurately represent the diurnal
363 cycle of precipitation.

364 The TRMM diurnal cycle of precipitation generally shows an increase of rainfall starting around
365 the noon with maximum reached at around 18:00 local solar time (LST) (Fig. 5). The ERAINT
366 diurnal cycle is completely out of the phase over all subregions with the occurrence of maximum
367 precipitation intensity around local noon. A common feature of ERAINT is an overestimation of
368 precipitation around local noon and an underestimation during the rest of the day.

369 HCLIM-ALADIN shows exactly the same behaviour as ERAINT. Both configurations of RCA4
370 simulate the diurnal cycle of precipitation more accurately compared to ERAINT and
371 HCLIM-ALADIN. The phase of the diurnal cycle, in general, is pretty well captured over all
372 four subregions. In terms of precipitation intensity RCA4 underestimates rainfall from afternoon
373 to morning over West (Fig. 5b,c) and Central Africa (Fig. 5j,k). Reducing mixing in the
374 boundary layer results in flattening of the diurnal cycle over West Africa (Fig. 5b, c) while there
375 are almost no changes over Central Africa (Fig. 5j, k). RCA4-v1 very well simulates the diurnal
376 cycle over Eastern Africa with only some underestimation in early morning and afternoon (Fig.
377 5f). RCA4-v4 improves rainfall intensity in early morning but at the same time shows a slightly

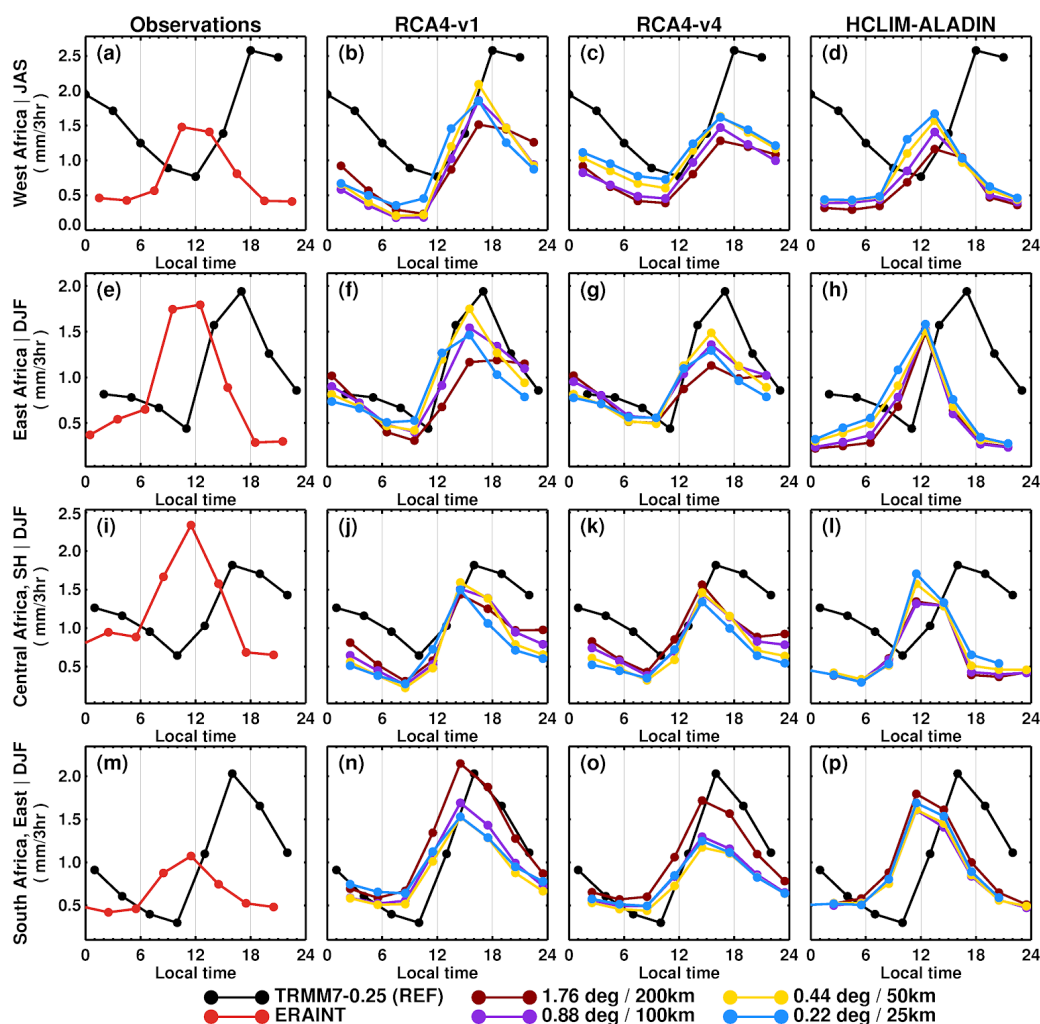


378 larger underestimation in afternoon than RCA4-v1 (Fig. 5g). Over Southern Africa the RCA4
379 simulations at 200km are the closest to the observation (Fig. 5n,o) while the simulations at
380 higher resolutions underestimate the amplitude of the diurnal cycle in the afternoon.
381 Figure 5 clearly shows that the phase of the diurnal cycle of precipitation in Africa does not
382 depend on resolution but instead depends on model formulation. Both ERAINT, with the Tiedtke
383 convection scheme (Tiedtke, 1989), and HCLIM-ALADIN with the Bougeault scheme
384 (Bougeault, 1985) trigger precipitation too early during the diurnal cycle while both
385 configurations of RCA4 with the same Kain–Fritsch (KF) scheme (Bechtold et al., 2001)
386 simulate much more realistic diurnal cycle. It has previously been shown that the KF scheme is
387 able to reproduce late afternoon rainfall peaks for the regions where moist convection is
388 governed by the local forcing, for example in the southeast US (Liang, 2004) and in the tropical
389 South America and Africa (e.g. Bechtold et al., 2004; Da Rocha et al., 2009). Nikulin et al.,
390 (2012) also found that a subset of RCMs that employ the KF scheme show an improved
391 representation of the phase of the diurnal cycle in Africa. Our results indicate that the impact of
392 resolution is only seen in the amplitude of the diurnal cycle. However, such impact is not
393 homogeneous across the subregions and the RCMs. For HCLIM-ALADIN, increasing resolution
394 lead to increasing rainfall intensity in all regions but southern Africa. RCA4 shows a similar
395 behaviour over West Africa, while there is a mixed response over Eastern and Central Africa.
396 These findings are in line with previous studies investigating resolution effects for GCMs
397 (Covey et al., 2016; Dirmeyer et al., 2012) and for RCMs (Walther et al., 2013). In coarser-scale
398 models (e.g >10km), increasing resolution only leads to changes in the magnitude, but not in the
399 phase of the diurnal cycle of precipitation over land.



400 Nevertheless, studies conducting sensitivity experiments using resolutions finer than 10 km do
 401 find improvements in the representation of the phase (Dirmeyer et al., 2012; Sato et al., 2009;
 402 Walther et al., 2013).

403 **Precipitation (pr) | 1998-2010 | land | Diurnal cycle**



404 **Figure 5.** Diurnal cycle of 3-hourly mean precipitation over the four subregions in observations/ERAINT
 405 and as simulated by RCA4 and HCLIM-ALADIN at the four different resolutions. Only land grid boxes
 406 are used for averaging over the subregions and only wet days with more than 1mm/day are taken for
 407 estimations of the diurnal cycle.

408



409

3.4 Frequency and intensity of daily precipitation

410 Figure 6 shows the empirical probability density function (PDF) of daily precipitation intensities
411 over the four subregions. The TRMM7-0.25 dataset, aggregated to the common 1.76° resolution
412 (TRMM7-1.76), as expected has a shorter right tail with no precipitation intensities larger than
413 100 mm day⁻¹ and higher frequency for lower intensities less than 25 mm day⁻¹ (Fig. 6a,e,i,m).
414 The two TRMM7 PDFs provide reference bounds for datasets with resolution between 0.25° and
415 1.76°. However, uncertainties in gridded daily precipitation products in Africa are large (Sylla et
416 al., 2013) and we take the TRMM bounds as an observational approximation focusing more on
417 differences in the simulated PDFs across the four resolutions. Over West, East and central Africa
418 ERAINT overestimates the frequency of low (< 10 mm day⁻¹) and extremely high (>150 mm
419 day⁻¹) intensities while it underestimates the frequency of precipitation intensities in between
420 (Fig. 6a,e,i), especially over West Africa (Fig. 6a). In southern Africa (Fig. 6m) ERAINT
421 represents the frequency of daily mean precipitation more accurately compared to the other three
422 regions but shows almost no events with more than 150 mm day⁻¹ in contrast to the
423 observations. Both RCMs, in general, have the same tendency to generate more higher-intensity
424 precipitation events with increasing resolution over all four subregions. In West Africa RCA4-v1
425 strongly underestimates the frequency of intensities with more than 20 mm day⁻¹ at 200, 100
426 and 50km (Fig. 6b). A substantial improvement appears only at 25km where the right tail of the
427 PDF extends up to 250 mm day⁻¹, although the frequency of precipitation events from about 50
428 to 150 mm day⁻¹ is still underestimated.

429



430 The RCA4-v4 configuration markedly reduces the RCA4-v1 biases and shows more realistic
431 PDFs at all four resolutions (Fig. 6c). The RCA4-v4 50km simulation generates precipitation
432 events up to 250 mm day⁻¹ strongly contrasting to the RCA4-v1 simulation at the same
433 resolution (no events more than 100 mm day⁻¹). However, RCA4-v4 overestimates frequencies
434 of high intensities at 25km. Such sharp difference between two configurations of RCA4 at the
435 same resolution shows that model formulation also plays an important role for accurately
436 reproducing daily precipitation. Over West Africa all HCLIM-ALADIN simulations
437 overestimates the frequency of low precipitation intensities (less than 10 mm day⁻¹) and
438 underestimates the frequency of intensities in the range of 10-150 mm day⁻¹ (Fig. 6d). Similar to
439 RCA4, higher resolution leads to more high-intensity precipitation events in the
440 HCLIM-ALADIN simulations.

441 However, RCA4 and HCLIM-ALADIN behave in a different way with increasing resolution.
442 Both RCMs change the PDFs by adding more higher-intensity precipitation events extending the
443 right-hand tail towards higher intensities. In addition, RCA4 also increases the frequency of
444 medium- and high-intensity events especially going from 50 to 25km. In eastern Africa both
445 RCA4 configurations reproduce the observed PDFs almost perfectly (Fig. 6f, g). All four
446 resolutions are located within the TRMM-1.76 and TRMM-0.25 boundaries and the coarsest and
447 finest resolutions coincides with the respective TRMM PDFs. Contrastingly, HCLIM-ALADIN
448 strongly underestimates the frequency of precipitation events with more than 20 mm day⁻¹ (Fig.
449 6h) over eastern Africa and even the highest 25km resolution is located below the coarse
450 TRMM-1.76 dataset. In central Africa both RCMs overestimate the occurrence of intensities less
451 than 20 mm day⁻¹ (Fig. 6j,k,l), especially HCLIM-ALADIN (Fig. 6l) and strongly underestimate



452 the frequency of higher-intensity events. The PDFs at all four resolutions for both RCMs are
453 located below the coarsest TRMM-1.76 PDF. We note that observational uncertainties in
454 precipitation are very large over central Africa and we should be careful in the interpretation of
455 Fig. 6j-l. Seasonal mean precipitation, for example, can differ by more than 50% across different
456 observational datasets (Washington et al., 2013). Additionally, the TRMM dataset is scaled by
457 the gauge-based GPCP precipitation product while almost no long-term gauges are available in
458 the region (Nikulin et al., 2012). In southern Africa RCA4 and HCLIM-ALADIN simulate the
459 precipitation PDFs pretty accurate (Fig. 6n-p). An interesting detail is that the 50km
460 HCLIM-ALADIN simulations shows higher frequency for intensities with more than 150 mm
461 day⁻¹ than the 25km simulation.

462 In general, we see the improvement of simulated daily rainfall intensities with increasing
463 resolution across the African continent. There are many studies showing a similar resolution-
464 dependent improvement over both complex terrains and flat regions (e.g. Chan et al., 2013;
465 Huang et al., 2016; Lindstedt et al., 2015; Olsson et al., 2015; Prein et al., 2016; Torma et al.,
466 2015a; Walther et al., 2013). Our results are in agreement with the above studies and confirm
467 increasing fidelity of simulated daily rainfall intensities with increasing resolution.

468

469

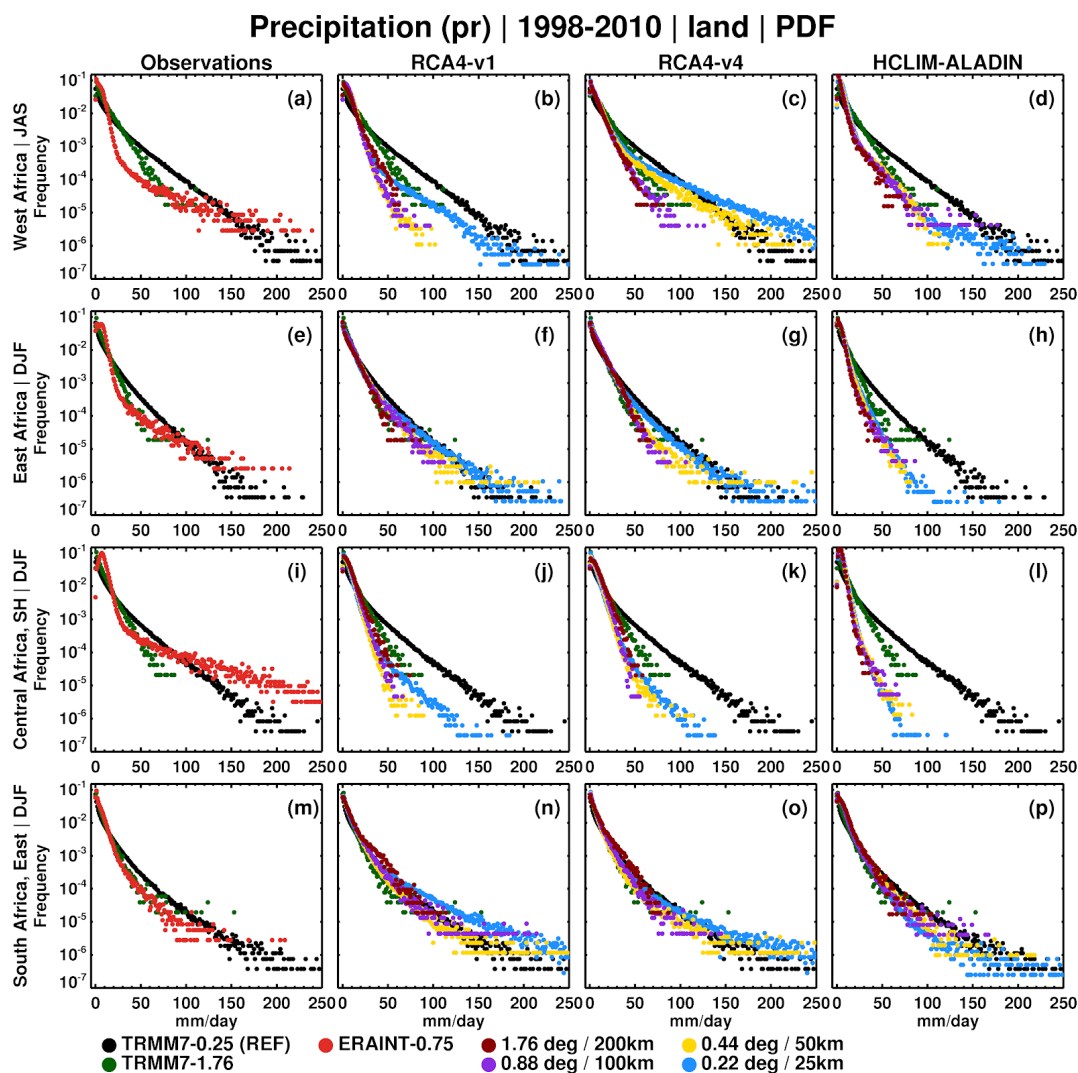
470

471

472



473



474 **Figure 6.** Probability distribution function of daily precipitation intensities pooled over the four subregions
 475 in observations/ERAINT and as simulated by RCA4 and HCLIM-ALADIN at the four different
 476 resolutions. TRMM7-1.76 represents TRMM7-0.25 aggregated from its native 0.25° resolution to 1.76°.
 477 A base-10 log scale is used for the frequency axis and the first bin (0-1 mm day⁻¹) is divided by 10. Only
 478 land grid boxes are used for pooling over the subregions.

479
 480

481



482

5 Summary and Conclusion

483 In this study we have investigated the impact of model formulation and spatial resolution on
484 simulated precipitation in Africa. A series of sensitivity, ERA-Interim reanalysis-driven
485 experiments, were conducted by applying two different RCMs (RCA4 and HCLIM-ALADIN) at
486 four resolutions (about 25, 50, 100 and 200 km). The 100km experiment, at resolution a bit
487 coarser than the driving ERA-Interim reanalysis, by default does not provide any
488 resolution-dependent added value while such added value is expected for the 50 and 25km
489 experiments. The 200km experiment is about 3 times upscaling of ERA-Interim to resolution of
490 many CMIP5 GCMs and should only be considered as a supplementary experiment since RCMs
491 do not aim to operate at such coarse resolution. In addition, to the two different RCMs, the
492 standard CORDEX configuration of RCA4 is supplemented by another configuration with
493 reduced mixing in the boundary layer. Such configuration was developed to deal with a strong
494 dry bias of RCA4 in Central Africa. Contrasting the two different RCMs and the two different
495 configurations of the same RCM at the four different resolutions allow us to separate the impact
496 of model formulation and resolution on simulated rainfall in Africa.
497 Even if the results often depend on region and season and a clear separation of the impact of
498 model formulation and resolution is not always straightforward, we found that model
499 formulation has the primary control over many aspects of the precipitation climatology in Africa.
500 The 100km no added value experiment shows that patterns of spatial biases in seasonal mean
501 precipitation are mostly defined by model formulation. These patterns are very different between
502 the driving ERA-Interim and RCMs, sometimes even with opposite sign, exemplified by the two



503 configurations of RCA4 in JAS (Fig. 1e-l). Resolution in general controls the magnitude of
504 biases and for both RCA4 and HCLIM-ALADIN higher resolution usually leads to an increase in
505 precipitation amount while preserving large-scale bias patterns. A side effect of such an increase
506 in precipitation amount is that an improvement in one region (e.g. reduction of dry biases) often
507 corresponds to a deterioration in another region (amplification of wet biases) as for
508 HCLIM-ALADIN in JAS (Fig. 1m-p). Nevertheless, on average the smallest biases in seasonal
509 means are found for the simulations at 50 and 25km resolution.

510 The impact of model formulation and resolution on the annual cycle of precipitation is mixed
511 and strongly depends on region and season. For example, in both West and Central Africa the
512 shape of the annual cycle for the 100km no added value experiment is different from ERAINT.
513 However, the impact of model formulation is opposite between these two regions. In West Africa
514 both RCMs deteriorate the ERAINT annual cycle by simulating a too early onset of the rainy
515 season. In contrast, over Central Africa, both models improve the ERAINT annual cycle by
516 reducing a strong wet bias and changing the unimodal annual cycle to a bimodal one similar to
517 the observations. The impact of resolution can also be different. In West and East Africa, higher
518 resolution (50 and 25km) leads to an improvement in the annual cycle (more realistic shape and
519 smaller biases). In contrast, over Central Africa, the 25km RCA4 simulations show the largest
520 biases while the HCLIM-ALADIN simulations at all four resolutions are almost similar. In
521 general, it is difficult to conclude on a common impact of model formulation and resolution on
522 the annual cycle.

523 The phase of the diurnal cycle in Africa is completely controlled by model formulation
524 (convection scheme) while its amplitude is a function of resolution. Both ERAINT and



525 HCLIM-ALADIN shows a too early precipitation maximum around noon while RCA4 simulates
526 a much more realistic diurnal cycle with an evening maximum. Higher resolution does not
527 change the phase of the diurnal cycle but its amplitude, although the impact of resolution on the
528 amplitude is mixed across the four subregions and time of the day.

529 A pronounced and well known impact of higher resolution on daily precipitation intensities is a
530 more realistic distribution of daily precipitation. Our results also show that higher resolution, in
531 general, improves the distribution of daily precipitation. This includes reduced overestimation of
532 the number of days with low precipitation intensities and reduced underestimation of the number
533 of days with high intensities. The latter results in extending the right-hand tail of the distribution
534 towards higher intensities similar to observations. This also means that at higher resolutions the
535 time mean climate (e.g. seasonal mean and annual cycle) is made up of more realistic
536 underpinning daily precipitation than at lower resolutions. It is also worth emphasizing that if
537 low resolution models are not able to simulate high rainfall days then it will be difficult for them
538 to say anything robust about projected climate changes in high rainfall events. However,
539 regionally, model formulation can also play an important role in the distribution of daily
540 precipitation. For example, in West Africa the 50km RCA4-v4 configuration with reduced
541 mixing in the boundary layer shows a remarkable improvement in the shape of the PDF (Fig. 1c)
542 compared to the standard RCA4-v1 configuration at the same resolution (Fig 1b). Moreover, the
543 RCA4-v4 configuration at 50 km shows almost the same PDF as RCA4-v1 at 25km. Such
544 contrast indicates that for daily precipitation intensities model formulation can have the same
545 impact as doubled resolution.



546 Improvements in simulated precipitation in high resolution RCMs relative to coarse-scale GCMs
547 are often attributed as being an resolution-dependent added value of downscaling. Our results
548 show that for Africa improvements are not always related to higher resolution but also to
549 different model formulation between the RCMs and their driving reanalysis. A common
550 framework for quantifying added value of downscaling is to evaluate some aspect of the climate
551 in high-resolution RCM simulations and in their coarse-resolution driving reanalysis or GCMs
552 over a historical period (Di Luca et al., 2015; e.g. Hong and Kanamitsu, 2014; Rummukainen,
553 2016). If the RCM simulations show smaller biases compared to reference observations than the
554 driving GCMs, one can conclude that RCMs provide an added value and vice versa. However,
555 such a framework does not separate the impact of different model formulation between RCMs
556 and their driving GCMs and higher resolution in the RCM simulations. Our results indicate that
557 improvements in RCM simulations may simply be related to different model formulation and not
558 necessarily to higher resolution. In general, model formulation related improvements cannot be
559 considered as an added value of downscaling as such improvements are strongly model
560 dependent and cannot be generalised.

561 Within commonly used RCM evaluation framework, e.g. the CORDEX evaluation experiment,
562 it is not straightforward, if possible at all, to isolate the impact of model formulation and
563 resolution in RCM simulations. We show that running RCMs at about the same resolution as a
564 driving reanalysis (e.g. ERAINT at about 80km or ERA5 at about 30km) helps to separate the
565 impacts of model formulation and higher resolution in dynamical downscaling. We propose that
566 such a simple additional experiment can be an integral part of the RCM evaluation framework in
567 order to elucidate the added value of downscaling.



568

Code availability

569 The analysis is done in MATLAB and IDL and codes can be provided by request as they are but
570 without support on implementing them in another computing environment.
571

Data availability

572 The ERA-Interim reanalysis is available at <https://apps.ecmwf.int/datasets/>, the GPCC dataset is
573 available at <https://www.dwd.de/EN/ourservices/gpcc/gpcc.html>, the CRU dataset is available at
574 <https://catalogue.ceda.ac.uk/uuid/5dca9487dc614711a3a933e44a933ad3>, the UDEL dataset is
575 available at http://climate.geog.udel.edu/~climate/html_pages/download.html, the TRMM
576 dataset is available at <https://pmm.nasa.gov/data-access/downloads/trmm>. The RCA4 and
577 HCLIM-ALADIN data can be provided by request.
578

Author contribution

579 MW performed RCA4 simulations and all the analysis and wrote the initial draft. GN developed
580 the experiment design and provided guidance for the analysis. EK and GN revised the initial
581 draft. CJ is responsible for setting up the new RCA4 configuration (v4). DB and DL are
582 responsible for performing the HCLIM-ALADIN simulations over Africa. All the authors
583 contributed with discussions and revisions.
584

Conflict of interest

585 There is no conflict of interest in this study.
586

Acknowledgements

587 This work was done with support from the FRACTAL (www.fractal.org.za) and AfriCultuReS
588 (<http://africultures.eu/>) projects. FRACTAL is part of the multi-consortia Future Climate for
589 Africa (FCFA) programme - jointly funded by the UK's Department for International
590 Development (DFID) and the Natural Environment Research Council (NERC). AfriCultuReS
591 has received funding from the European Union's Horizon 2020 research and innovation
592 programme under grant agreement No 774652. The authors thank the European Centre for
593 Medium-Range Weather Forecasts (ECMWF), the Global Precipitation Climatology Centre
594 (GPCC), the British Atmospheric Data Centre (BADC), the University of East Anglia (UEA),
595 the University of Delaware and the Goddard Space Flight Center (GSFC) for providing data. All



596 simulations were conducted on the supercomputer in the National Supercomputer Centre,
597 Linköping, Sweden.

598
599
600
601
602
603
604
605
606
607
608
609
610
611
612
613
614
615
616
617
618
619
620
621
622
623
624
625
626
627
628
629
630
631
632
633
634



635

Reference

- 636 Bechtold, P., Bazile, E., Guichard, F., Mascart, P. and Richard, E.: A mass-flux convection
637 scheme for regional and global models, *Q.J Royal Met. Soc.*, 127(573), 869–886, 2001.
- 638 Bechtold, P., Chaboureau, J. P., Beljaars, A., Betts, K., Köhler, M., Miller, M. and Redelsperger,
639 J. L.: The simulation of the diurnal cycle of convective precipitation over land in a global model,
640 *Quarterly Journal of the Royal Meteorological Society*, (130), 3119–3137, 2004.
- 641 Belušić, D., de Vries, H., Dobler, A., Landgren, O., Lind, P., Lindstedt, D., Pedersen, R. A.,
642 Sánchez-Perrino, J. C., Toivonen, E., van Ulft, B. and Others: HCLIM38: A flexible regional
643 climate model applicable for different climate zones from coarse to convection permitting scales,
644 *Geoscientific Model Development Discussion*, doi:10.5194/gmd-2019-151, 2019.
- 645 Bengtsson, L., Andrae, U., Aspeliën, T., Batrak, Y., Calvo, J., de Rooy, W., Gleeson, E.,
646 Hansen-Sass, B., Homleid, M., Hortal, M., Ivarsson, K.-I., Lenderink, G., Niemelä, S., Nielsen,
647 K. P., Onville, J., Rontu, L., Samuelsson, P., Muñoz, D. S., Subias, A., Tijm, S., Toll, V., Yang, X.
648 and Køltzow, M. Ø.: The HARMONIE–AROME Model Configuration in the ALADIN–HIRLAM
649 NWP System, *Mon. Weather Rev.*, 145(5), 1919–1935, 2017.
- 650 Berg, P., Döscher, R. and Koenigk, T.: Impacts of using spectral nudging on regional climate
651 model RCA4 simulations of the Arctic, *Geoscientific Model Development*, 6(3), 849–859, 2013.
- 652 Bougeault, P.: A Simple Parameterization of the Large-Scale Effects of Cumulus Convection,
653 *Mon. Weather Rev.*, 113(12), 2108–2121, 1985.
- 654 Caron, L.-P., Jones, C. G. and Winger, K.: Impact of resolution and downscaling technique in
655 simulating recent Atlantic tropical cyclone activity, *Clim. Dyn.*, 37(5), 869–892, 2011.
- 656 Castro, C. L.: Dynamical downscaling: Assessment of value retained and added using the
657 Regional Atmospheric Modeling System (RAMS), *J. Geophys. Res.*, 110(D5), 681, 2005.
- 658 Challinor, A., Wheeler, T., Garforth, C., Craufurd, P. and Kassam, A.: Assessing the vulnerability
659 of food crop systems in Africa to climate change, *Clim. Change*, 83(3), 381–399, 2007.
- 660 Chan, S. C., Kendon, E. J., Fowler, H. J., Blenkinsop, S., Ferro, C. A. T. and Stephenson, D. B.:
661 Does increasing the spatial resolution of a regional climate model improve the simulated daily
662 precipitation?, *Clim. Dyn.*, 41(5), 1475–1495, 2013.
- 663 Collazo, S., Lhotka, O., Rusticucci, M. and Kysell, J.: Capability of the SMHI-RCA4 RCM
664 driven by the ERA-Interim reanalysis to simulate heat waves in Argentina, *Int. J. Climatol.*,
665 38(1), 483–496, 2018.
- 666 Covey, C., Gleckler, P. J., Doutriaux, C., Williams, D. N., Dai, A., Fasullo, J., Trenberth, K. and
667 Berg, A.: Metrics for the Diurnal Cycle of Precipitation: Toward Routine Benchmarks for Climate
668 Models, *J. Clim.*, 29(12), 4461–4471, 2016.
- 669 Dai, A.: Precipitation Characteristics in Eighteen Coupled Climate Models, *J. Clim.*, 19(18),



- 670 4605–4630, 2006.
- 671 Dai, A. and Trenberth, K. E.: The Diurnal Cycle and Its Depiction in the Community Climate
672 System Model, *J. Clim.*, 17(5), 930–951, 2004.
- 673 Dai, A., Lin, X. and Hsu, K.-L.: The frequency, intensity, and diurnal cycle of precipitation in
674 surface and satellite observations over low- and mid-latitudes, *Clim. Dyn.*, 29(7), 727–744,
675 2007.
- 676 Daniel, M., Lemonsu, A., Déqué, M., Somot, S., Alias, A. and Masson, V.: Benefits of explicit
677 urban parameterization in regional climate modeling to study climate and city interactions, *Clim.*
678 *Dyn.*, 52(5), 2745–2764, 2019.
- 679 Da Rocha, R. P., Morales, C. A., Cuadra, S. V. and Ambrizzi, T.: Precipitation diurnal cycle and
680 summer climatology assessment over South America: An evaluation of Regional Climate Model
681 version 3 simulations, *Journal of Geophysical Research*, doi:10.1029/2008JD010212, 2009.
- 682 Dee, D. P., Uppala, S. M., Simmons, A. J., Berrisford, P., Poli, P., Kobayashi, S., Andrae, U.,
683 Balmaseda, M. A., Balsamo, G., Bauer, d. P. and Others: The ERA-Interim reanalysis:
684 Configuration and performance of the data assimilation system, *Quart. J. Roy. Meteor. Soc.*,
685 137(656), 553–597, 2011.
- 686 Diaconescu, E. P. and Laprise, R.: Can added value be expected in RCM-simulated large
687 scales?, *Clim. Dyn.*, 41(7), 1769–1800, 2013.
- 688 Di Luca, A., de Elía, R. and Laprise, R.: Potential for added value in precipitation simulated by
689 high-resolution nested Regional Climate Models and observations, *Clim. Dyn.*,
690 doi:10.1007/s00382-011-1068-3, 2012.
- 691 Di Luca, A., de Elía, R. and Laprise, R.: Challenges in the Quest for Added Value of Regional
692 Climate Dynamical Downscaling, *Current Climate Change Reports*, 1(1), 10–21, 2015.
- 693 Dirmeyer, P. A., Cash, B. A., Kinter, J. L., Jung, T., Marx, L., Satoh, M., Stan, C., Tomita, H.,
694 Towers, P., Wedi, N., Achuthavarier, D., Adams, J. M., Altshuler, E. L., Huang, B., Jin, E. K. and
695 Manganello, J.: Simulating the diurnal cycle of rainfall in global climate models: resolution
696 versus parameterization, *Clim. Dyn.*, 39(1), 399–418, 2012.
- 697 Dosio, A., Panitz, H.-J., Schubert-Frisius, M. and Lüthi, D.: Dynamical downscaling of CMIP5
698 global circulation models over CORDEX-Africa with COSMO-CLM: evaluation over the present
699 climate and analysis of the added value, *Clim. Dyn.*, 44(9), 2637–2661, 2015.
- 700 Fekete, B. M., Vörösmarty, C. J., Roads, J. O. and Willmott, C. J.: Uncertainties in Precipitation
701 and Their Impacts on Runoff Estimates, *J. Clim.*, 17(2), 294–304, 2004.
- 702 Flato, G., Marotzke, J., Abiodun, B., Braconnot, P., Chou, S. C., Collins, W., Cox, P., Driouech,
703 F., Emori, S., Eyring, V., Forest, C., Gleckler, P., Guilyardi, E., Jakob, C., Kattsov, V., Reason, C.
704 and Rummukainen, M.: Evaluation of Climate Models, *Climate Change 2013: The Physical
705 Science Basis. Contribution of Working Group I to the Fifth Assessment Report of the
706 Intergovernmental Panel on Climate Change*, 741–866, 2013.



- 707 Giorgi, F. and Gao, X.-J.: Regional earth system modeling: review and future directions,
708 *Atmospheric and Oceanic Science Letters*, 11(2), 189–197, 2018.
- 709 Giorgi, F. and Mearns, L. O.: Approaches to the simulation of regional climate change: A review,
710 *Rev. Geophys.*, 29(2), 191, 1991.
- 711 Giorgi, F., Jones, C., Asrar, G. R. and Others: Addressing climate information needs at the
712 regional level: the CORDEX framework, *WMO Bull.*, 58(3), 175, 2009.
- 713 Gruber, A., Su, X., Kanamitsu, M. and Schemm, J.: The Comparison of Two Merged Rain
714 Gauge–Satellite Precipitation Datasets, *Bull. Am. Meteorol. Soc.*, 81(11), 2631–2644, 2000.
- 715 Harris, I., Jones, P. D., Osborn, T. J. and Lister, D. H.: Updated high-resolution grids of monthly
716 climatic observations--the CRU TS3. 10 Dataset, *Int. J. Climatol.*, 34(3), 623–642, 2014.
- 717 Hong, S. Y. and Kanamitsu, M.: Dynamical downscaling: Fundamental issues from an NWP
718 point of view and recommendations, *Asia-Pacific Journal of Atmospheric Sciences*, 50(1),
719 83–104, 2014.
- 720 Huang, X., Rhoades, A. M., Ullrich, P. A. and Zarzycki, C. M.: An evaluation of the
721 variable-resolution CESM for modeling California's climate, *Journal of Advances in Modeling
722 Earth Systems*, 8(1), 345–369, 2016.
- 723 Huffman, G. J., Bolvin, D. T., Nelkin, E. J., Wolff, D. B., Adler, R. F., Gu, G., Hong, Y., Bowman,
724 K. P. and Stocker, E. F.: The TRMM Multisatellite Precipitation Analysis (TMPA): Quasi-Global,
725 Multiyear, Combined-Sensor Precipitation Estimates at Fine Scales, *J. Hydrometeorol.*, 8(1),
726 38–55, 2007.
- 727 Iqbal, W., Syed, F. S., Sajjad, H., Nikulin, G., Kjellström, E. and Hannachi, A.: Mean climate and
728 representation of jet streams in the CORDEX South Asia simulations by the regional climate
729 model RCA4, *Theor. Appl. Climatol.*, 129(1), 1–19, 2017.
- 730 Jeong, J.-H., Walther, A., Nikulin, G., Chen, D. and Jones, C.: Diurnal cycle of precipitation
731 amount and frequency in Sweden: observation versus model simulation, *Tellus Ser. A Dyn.
732 Meteorol. Oceanogr.*, 63(4), 664–674, 2011.
- 733 Jiao, Y. and Jones, C.: Comparison Studies of Cloud- and Convection-Related Processes
734 Simulated by the Canadian Regional Climate Model over the Pacific Ocean, *Mon. Weather
735 Rev.*, 136(11), 4168–4187, 2008.
- 736 Jones, C., Giorgi, F. and Asrar, G.: The Coordinated Regional Downscaling Experiment:
737 CORDEX--an international downscaling link to CMIP5, CLIVAR exchanges, 16(2), 34–40, 2011.
- 738 Jones, C. G., Willén, U., Ullerstig, A. and Hansson, U.: The Rossby Centre Regional
739 Atmospheric Climate Model part I: model climatology and performance for the present climate
740 over Europe, *Ambio*, 33(4-5), 199–210, 2004.
- 741 Jones, P. W.: First- and Second-Order Conservative Remapping Schemes for Grids in Spherical
742 Coordinates, *Mon. Weather Rev.*, 127(9), 2204–2210, 1999.
- 743 Kim, J., Waliser, D. E., Mattmann, C. A., Goodale, C. E., Hart, A. F., Zimdars, P. A., Crichton, D.



- 744 J., Jones, C., Nikulin, G., Hewitson, B., Jack, C., Lennard, C. and Favre, A.: Evaluation of the
745 CORDEX-Africa multi-RCM hindcast: systematic model errors, *Clim. Dyn.*, 42(5), 1189–1202,
746 2014.
- 747 Kjellström, E., Bärring, L., Gollvik, S., Hansson, U., Jones, C., Samuelsson, P., Ullerstig, A.,
748 Willén, U. and Wyser, K.: A 140-year simulation of European climate with the new version of the
749 Rossby Centre regional atmospheric climate model (RCA3), [online] Available from:
750 <http://www.diva-portal.org/smash/record.jsf?pid=diva2:947602> (Accessed 19 November 2018),
751 2005.
- 752 Kjellström, E., Bärring, L., Nikulin, G., Nilsson, C., Persson, G. and Strandberg, G.: Production
753 and use of regional climate model projections - A Swedish perspective on building climate
754 services, *Clim Serv*, 2-3, 15–29, 2016.
- 755 Kjellström, E., Nikulin, G., Strandberg, G., Christensen, O. B., Jacob, D., Keuler, K., Lenderink,
756 G., van Meijgaard, E., Schär, C., Somot, S., Sørland, S. L., Teichmann, C. and Vautard, R.:
757 European climate change at global mean temperature increases of 1.5 and 2 °C above
758 pre-industrial conditions as simulated by the EURO-CORDEX regional climate models, *Earth
759 System Dynamics*, 9(2), 459–478, 2018.
- 760 Koenigk, T., Berg, P. and Döscher, R.: Arctic climate change in an ensemble of regional
761 CORDEX simulations, *Polar Res.*, 34(1), 24603, 2015.
- 762 Kotlarski, S., Lüthi, D. and Schär, C.: The elevation dependency of 21st century European
763 climate change: an RCM ensemble perspective, *Int. J. Climatol.*, 35(13), 3902–3920, 2015.
- 764 Laprise, R.: Regional climate modelling, *J. Comput. Phys.*, 227(7), 3641–3666, 2008.
- 765 Laprise, R., Hernández-Díaz, L., Tete, K., Sushama, L., Šeparović, L., Martynov, A., Winger, K.
766 and Valin, M.: Climate projections over CORDEX Africa domain using the fifth-generation
767 Canadian Regional Climate Model (CRCM5), *Clim. Dyn.*, 41(11), 3219–3246, 2013.
- 768 Legates, D. R. and Willmott, C. J.: Mean seasonal and spatial variability in global surface air
769 temperature, *Theor. Appl. Climatol.*, 41(1), 11–21, 1990.
- 770 Lenderink, G. and Holtslag, A. A. M.: An updated length-scale formulation for turbulent mixing in
771 clear and cloudy boundary layers, *Quart. J. Roy. Meteor. Soc.*, 130(604), 3405–3427, 2004.
- 772 Liang, X.-Z.: Regional climate model simulation of summer precipitation diurnal cycle over the
773 United States, *Geophys. Res. Lett.*, 31(24), 2033, 2004.
- 774 Lindstedt, D., Lind, P., Kjellström, E. and Jones, C.: A new regional climate model operating at
775 the meso-gamma scale: Performance over Europe, *Tellus Ser. A Dyn. Meteorol. Oceanogr.*,
776 67(1), doi:10.3402/tellusa.v67.24138, 2015.
- 777 Lucas-Picher, P., Laprise, R. and Winger, K.: Evidence of added value in North American
778 regional climate model hindcast simulations using ever-increasing horizontal resolutions, *Clim.
779 Dyn.*, 48(7), 2611–2633, 2017.
- 780 Masson, V., Moigne, P. L., Martin, E., Faroux, S., Alias, A., Alkama, R., Belamari, S., Barbu, A.,



- 781 Boone, A., Bouyssel, F., Brousseau, P., Brun, E., Calvet, J.-C., Carrer, D., Decharme, B., Delire,
782 C., Donier, S., Essaouini, K., Gibelin, A.-L., Giordani, H., Habets, F., Jidane, M., Kerdraon, G.,
783 Kourzeneva, E., Lafaysse, M., Lafont, S., Lebeaupin Brossier, C., Lemonsu, A., Mahfouf, J.-F.,
784 Marguinaud, P., Mokhtari, M., Morin, S., Pigeon, G., Salgado, R., Seity, Y., Taillefer, F., Tanguy,
785 G., Tulet, P., Vincendon, B., Vionnet, V. and Voldoire, A.: The SURFEXv7.2 land and ocean
786 surface platform for coupled or offline simulation of earth surface variables and fluxes,
787 *Geoscientific Model Development*, 6(4), 929–960, 2013.
- 788 Moufouma-Okia, W. and Jones, R.: Resolution dependence in simulating the African
789 hydroclimate with the HadGEM3-RA regional climate model, *Clim. Dyn.*, 44(3), 609–632, 2015.
- 790 Munday, C. and Washington, R.: Systematic Climate Model Rainfall Biases over Southern
791 Africa: Links to Moisture Circulation and Topography, *J. Clim.*, 31(18), 7533–7548, 2018.
- 792 Nikulin, G., Jones, C., Giorgi, F., Asrar, G., Büchner, M., Cerezo-Mota, R., Christensen, O. B.,
793 Déqué, M., Fernandez, J., Hänsler, A., van Meijgaard, E., Samuelsson, P., Sylla, M. B. and
794 Sushama, L.: Precipitation climatology in an ensemble of CORDEX-Africa regional climate
795 simulations, *J. Clim.*, 25(18), 6057–6078, 2012.
- 796 Nikulin, G., Lennard, C., Dosio, A., Kjellström, E., Chen, Y., Hänsler, A., Kupiainen, M., Laprise,
797 R., Mariotti, L., Maule, C. F., van Meijgaard, E., Panitz, H.-J., Scinocca, J. F. and Somot, S.: The
798 effects of 1.5 and 2 degrees of global warming on Africa in the CORDEX ensemble, *Environ.*
799 *Res. Lett.*, 13(6), 065003, 2018.
- 800 Olsson, J., Berg, P. and Kawamura, A.: Impact of RCM Spatial Resolution on the Reproduction
801 of Local, Subdaily Precipitation, *J. Hydrometeorol.*, 16(2), 534–547, 2015.
- 802 Panitz, H.-J., Dosio, A., Büchner, M., Lüthi, D. and Keuler, K.: COSMO-CLM (CCLM) climate
803 simulations over CORDEX-Africa domain: analysis of the ERA-Interim driven simulations at
804 0.44° and 0.22° resolution, *Clim. Dyn.*, 42(11), 3015–3038, 2014.
- 805 Prein, A. F., Gobiet, A., Truhetz, H., Keuler, K., Goergen, K., Teichmann, C., Maule, C. F., Van
806 Meijgaard, E., Déqué, M., Nikulin, G. and Robert, Vautard, Augustin, Colette, Erik, Kjellström,
807 Daniela Jacob: Precipitation in the EURO-CORDEX 0.11° and 0.44° simulations: high
808 resolution, high benefits?, *Clim. Dyn.*, 46(1-2), 383–412, 2016.
- 809 Räisänen, J., Hansson, U., Ullerstig, A., Döscher, R., Graham, L. P., Jones, C., Meier, H. E. M.,
810 Samuelsson, P. and Willén, U.: European climate in the late twenty-first century: regional
811 simulations with two driving global models and two forcing scenarios, *Clim. Dyn.*, 22(1), 13–31,
812 2004.
- 813 Rummukainen, M.: State-of-the-art with regional climate models, *Wiley Interdiscip. Rev. Clim.*
814 *Change*, 1(1), 82–96, 2010.
- 815 Rummukainen, M.: Added value in regional climate modeling, *WIREs Clim Change*, 7(1),
816 145–159, 2016.
- 817 Rummukainen, M., Räisänen, J., Bringfelt, B., Ullerstig, A., Omstedt, A., Willén, U., Hansson, U.
818 and Jones, C.: A regional climate model for northern Europe: model description and results from



- 819 the downscaling of two GCM control simulations, *Clim. Dyn.*, 17(5), 339–359, 2001.
- 820 Samuelsson, P., Jones, C. G., Willén, U., Ullerstig, A., Gollvik, S., Hansson, U., Jansson, E.,
821 Kjellström, C., Nikulin, G. and Wyser, K.: The Rossby Centre Regional Climate model RCA3:
822 model description and performance, *Tellus Ser. A Dyn. Meteorol. Oceanogr.*, 63(1), 4–23, 2011.
- 823 Sato, T., Miura, H., Satoh, M., Takayabu, Y. N. and Wang, Y.: Diurnal Cycle of Precipitation in
824 the Tropics Simulated in a Global Cloud-Resolving Model, *J. Clim.*, 22(18), 4809–4826, 2009.
- 825 Schneider, U., Becker, A., Finger, P., Meyer-Christoffer, A., Ziese, M. and Rudolf, B.: GPCP's
826 new land surface precipitation climatology based on quality-controlled in situ data and its role in
827 quantifying the global water cycle, *Theor. Appl. Climatol.*, 115(1), 15–40, 2014.
- 828 Sørland, S. L., Schär, C., Lüthi, D. and Kjellström, E.: Bias patterns and climate change signals
829 in GCM-RCM model chains, *Environ. Res. Lett.*, 13(7), 074017, 2018.
- 830 Sylla, M. B., Giorgi, F., Coppola, E. and Mariotti, L.: Uncertainties in daily rainfall over Africa:
831 assessment of gridded observation products and evaluation of a regional climate model
832 simulation: UNCERTAINTIES IN OBSERVED AND SIMULATED DAILY RAINFALL OVER
833 AFRICA, *Int. J. Climatol.*, 33(7), 1805–1817, 2013.
- 834 Tamoffo, A. T., Moufouma-Okia, W., Dosio, A., James, R., Pokam, W. M., Vondou, D. A.,
835 Fotso-Nguemo, T. C., Guenang, G. M., Kamsu-Tamo, P. H., Nikulin, G., Longandjo, G.-N.,
836 Lennard, C. J., Bell, J.-P., Takong, R. R., Haensler, A., Tchotchou, L. A. D. and Nouayou, R.:
837 Process-oriented assessment of RCA4 regional climate model projections over the Congo Basin
838 under 1.5°C and 2°C global warming levels: influence of regional moisture fluxes, *Clim. Dyn.*,
839 doi:10.1007/s00382-019-04751-y, 2019.
- 840 Tangang, F., Supari, S., Chung, J. X., Cruz, F., Salimun, E., Ngai, S. T., Juneng, L.,
841 Santisirisomboon, J., Santisirisomboon, J., Ngo-Duc, T., Phan-Van, T., Narisma, G., Singhruck,
842 P., Gunawan, D., Aldrian, E., Sopaheluwakan, A., Nikulin, G., Yang, H., Remedio, A. R. C., Sein,
843 D. and Hein-Griggs, D.: Future changes in annual precipitation extremes over Southeast Asia
844 under global warming of 2°C, *APN Science Bulletin*, 8(1), doi:10.30852/sb.2018.436, 2018.
- 845 Temperton, C., Hortal, M. and Simmons, A.: A two-time-level semi-Lagrangian global spectral
846 model, *Q. J. Royal Met. Soc.*, 127(571), 111–127, 2001.
- 847 Termonia, P., Fischer, C., Bazile, E., Bouyssel, F., Brožková, R., Bénard, P., Bochenek, B.,
848 Degrauwe, D., Derková, M., El Khatib, R. and Others: The ALADIN System and its canonical
849 model configurations AROME CY41T1 and ALARO CY40T1, *Geoscientific Model Development*,
850 11, 257–281, 2018.
- 851 Tiedtke, M.: A Comprehensive Mass Flux Scheme for Cumulus Parameterization in Large-Scale
852 Models, *Mon. Weather Rev.*, 117(8), 1779–1800, 1989.
- 853 Torma, C., Giorgi, F. and Coppola, E.: Added value of regional climate modeling over areas
854 characterized by complex terrain-Precipitation over the Alps, *J. Geophys. Res. D: Atmos.*,
855 120(9), 3957–3972, 2015a.
- 856 Torma, C., Giorgi, F. and Coppola, E.: Added value of regional climate modeling over areas



- 857 characterized by complex terrain-Precipitation over the Alps: ADDED VALUE OF RCM OVER
858 COMPLEX TERRAIN, *J. Geophys. Res. D: Atmos.*, 120(9), 3957–3972, 2015b.
- 859 Undén, P., Rontu, L., Jäärvinen, H., Lynch, P. and Calvo, J.: HIRLAM-5 scientific documentation,
860 SMHI, SMHI, SE-601 76 Norrköping., 2002.
- 861 Van der Linden, P. and Mitchell, E., JFB: ENSEMBLES: Climate change and its
862 impacts-Summary of research and results from the ENSEMBLES project, 2009.
- 863 Walther, A., Jeong, J.-H., Nikulin, G., Jones, C. and Chen, D.: Evaluation of the warm season
864 diurnal cycle of precipitation over Sweden simulated by the Rossby Centre regional climate
865 model RCA3, *Atmos. Res.*, 119, 131–139, 2013.
- 866 Wang, J. and Kotamarthi, V. R.: Downscaling with a nested regional climate model in
867 near-surface fields over the contiguous United States: WRF dynamical downscaling, *J.*
868 *Geophys. Res. D: Atmos.*, 119(14), 8778–8797, 2014.
- 869 Washington, R., James, R., Pearce, H., Pokam, W. M. and Moufouma-Okia, W.: Congo Basin
870 rainfall climatology: can we believe the climate models?, *Philos. Trans. R. Soc. Lond. B Biol.*
871 *Sci.*, 368(1625), 20120296, 2013.
- 872 Wu, M., Schurgers, G., Rummukainen, M., Smith, B., Samuelsson, P., Jansson, C., Siltberg, J.
873 and May, W.: Vegetation-climate feedbacks modulate rainfall patterns in Africa under future
874 climate change, *Earth System Dynamics*, 7(3), 627–647, 2016.
- 875 Wu, M., Schurgers, G., Ahlström, A., Rummukainen, M., Miller, P. A., Smith, B. and May, W.:
876 Impacts of land use on climate and ecosystem productivity over the Amazon and the South
877 American continent, *Environ. Res. Lett.*, 12(5), 054016, 2017.
- 878 Xue, Y., Janjic, Z., Dudhia, J., Vasic, R. and De Sales, F.: A review on regional dynamical
879 downscaling in intraseasonal to seasonal simulation/prediction and major factors that affect
880 downscaling ability, *Atmos. Res.*, 147-148, 68–85, 2014.
- 881 Zhang, W., Jansson, C., Miller, P. A., Smith, B. and Samuelsson, P.: Biogeophysical feedbacks
882 enhance the Arctic terrestrial carbon sink in regional Earth system dynamics, *Biogeosciences*,
883 11(19), 5503–5519, 2014.
- 884